

Time-Resolved Kinetic Studies on Quenching of $\text{HCF}(\tilde{A}^1A'')$ by Alkane and Alcohol Molecules

Xueliang Yang, Weiqing Zhang, Min Ji, Yang Chen, and Congxiang Chen*

Open Laboratory of Bond-selective Chemistry, Chinese Academy of Sciences, Department of Chemical Physics, University of Science and Technology of China, Hefei 230026

Received: January 24, 2005; In Final Form: April 21, 2005

$\text{HCF}(\tilde{X}^1A')$ radicals were produced by laser photolysis of CHFBr_2 at 213 nm and were electronically excited from the ground state to $\tilde{A}^1A''(030)$ at 492.7 nm with a dye laser pumped by a Nd:YAG laser. With the analysis of the lifetime of the time-resolved total fluorescence signals collected in the reaction cell where the total pressure was fixed to be 14.0 Torr, the quenching data of $\text{HCF}(\tilde{A}^1A'')$ by alkane and alcohol molecules at room temperature were derived from variation of pseudo-first-order rate constant with different quencher pressures. It is found that the quenching rate constants are close to the collision rate constants ($10^{-10} \text{ cm}^3 \text{ molecule}^{-1} \text{ s}^{-1}$), indicating the long-range attractive forces between the collision partners play an important role in the entrance channel of quenching process. Several kinetic models were applied to analyze the mechanism of the quenching process. The complex formation cross sections are calculated with the collision complex model. Correlations of the quenching rate constant for the removal of the $\text{HCF}(\tilde{A}^1A'')$ state with ionization potential of the quenching partners show that the insertion reactive mechanism is probably the dominant reaction channel, which is analogous to the behaviors of other three-atom carbenes in corresponding electronic states.

Introduction

Carbenes have been studied extensively for many years and the interest in this group of molecules has continued unabated to date due to their importance in synthetic organic chemistry, interstellar chemistry, pharmaceuticals, and combustion processes.^{1–3} The interest in, and application of these molecules originates from their electronic structure. The two nonbonding valence electrons on the carbon may be either paired in the same orbital in the “carbene” structure (the ground state of HCF , HCCl , HCBBr , CF_2 , CFCl , CFBr , CCl_2 , CClBr , and CBr_2), or in two different orbitals, the “biradical” structure (the ground state of CH_2 and CHI , and the electronically excited states of carbenes). Their chemical properties are vastly different for each configuration. Although both kinds of species are very reactive, carbenes are more stable and retain stereospecificity in organic reactions, whereas the biradicals are extremely reactive and do not retain stereospecificity.

Carbenes usually behave as strong electrophiles,⁴ and their singlet species undergo direct insertion reactions into single bonds^{2,5–9} and addition to multiple bonds^{10–12} by collision with various molecules. A considerable number of empirical methods and ab initio molecular orbital calculations have been performed to explain both insertion^{13–16} and cycloaddition reactions.^{17–21} As the smallest carbene with a singlet ground state, HCF is expected to serve as a convenient model for understanding the spectroscopy, photochemistry, and reactivity of larger analogues, such as HCCl , HCBBr , CF_2 , CFCl , CFBr , CCl_2 , CClBr , and CBr_2 . Since Merer and Travis²² reported the first rotationally resolved absorption spectra of HCF between 430 and 600 nm in the flash photolysis of CHFBr_2 in 1966, there have been numerous investigations on the spectroscopy of HCF ^{22–40} and the reaction

dynamics of the ground state with atomic species (N, H, O),^{41–44} inorganic molecules (NO , NO_2 , N_2O , O_2 , and O_3),^{41,44–49} and alkenes.^{10–12,50}

In this work, the quenching processes of $\text{HCF}(\tilde{A}^1A'')$ by alkane and alcohol molecules are presented. The quenching rate constants and cross sections have been experimentally determined at room temperature ($T = 293 \text{ K}$).

Experimental Section

The pulsed laser photolysis/laser-induced fluorescence (LP-LIF) experiments were performed in a stainless steel flow reactor, which is similar to those described in detail previously.^{51–54} Briefly, HCF radicals were generated from the photolysis of CHFBr_2 with the softly focused 213 nm irradiation of a frequency-quintupled Nd:YAG laser (New wave, repetition rate of 10 Hz). A 50 cm focal length quartz lens focused the beam into the center of the reaction cell. After a time delay, the ground-state $\text{HCF}(\tilde{X}^1A')$ was electronically excited to $\tilde{A}^1A''(030)$ at 492.7 nm using a dye laser beam (Sirah) pumped by Nd:YAG laser (Spectra physics, GCR-170, repetition rate of 10 Hz). The excitation laser and the photolysis laser beams overlapped in the reaction cell collinearly in a counters propagating way. Also, the typical output pulse energies of them were 2 and 3 mJ, respectively. To minimize scattering light, the laser beams were passed through a set of special light baffles. The fluorescence signals of the excited HCF were collected by a photomultiplier (GDB56, Beijing) through a cutoff filter with wavelength longer than 550 nm and inputted into a digital storage oscilloscope (TDS380, Tektronix) or a transient digitizer and averaged with a computer data acquisition system over 512 laser shots. A multichannel digital delay generator (Stanford Research DG535) controlled the time delay between the photolysis laser and the excitation dye laser beam.

* To whom correspondence should be addressed. Tel: +86-551-3607736/3607865. Fax: +86-551-3602969. E-mail: cxchen@ustc.edu.cn.

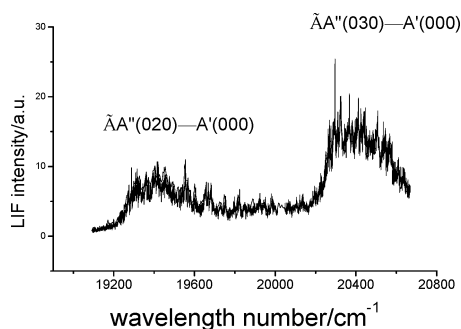


Figure 1. LIF excitation spectrum of HCF obtained at 25 μ s delay after 213 nm photolysis of CHFBr₂ under the pressure of 14.0 Torr at 293 K.

In a typical experiment, the premixed gas sample containing CHFBr₂ molecule as the HCF radical precursor and the quenchers mixed with Ar were supplied from different reservoirs and controlled by an individually calibrated mass flow controller (D07-7A/3M, Beijing) and slowly passed through the reaction cell. In the reaction cell, the typical concentration of CHFBr₂ was about 6.0×10^{13} molecule cm⁻³, whereas the concentrations of alkane and alcohol molecules varied in the range from 1.0×10^{14} molecule cm⁻³ up to 3.0×10^{15} molecule cm⁻³. The total pressure in the chamber was about 14.0 Torr. The HCF radicals generated from the photolysis of the precursor are vibrationally and rotationally hot. The Ar buffer gas in the reaction mixture serves not only to relax the nascent quantum state distributions of the HCF radicals but also to slow the diffusion of molecules out of the detection region.

Materials. In this work, methane (Nanjing gas, 99.9%), ethane (Nanjing gas, 99.99%), propane (Nanjing gas, 99.9%), *n*-butane (Nanjing gas, 99.9%), *n*-pentane (Tianjin, >99.9%), *n*-hexane (Tianjin, >99.9%), *n*-heptane (Shanghai, >99.5%), *n*-octane (Shanghai, >97.5%), methanol (Jiangsu, >99.5%), ethanol (Shanghai, >99.5%), *n*-propanol (Shanghai, >99.0%), *n*-butanol (Shanghai, >99.5%), and CHFBr₂ (Aldrich Chemical Co., 98.0%). All of the samples were purified by repeated freeze–pump–thaw cycles in liquid nitrogen. Ar (Nanjing gas, 99.999%) was used from cylinder without further purification.

Results

A portion of the LIF excitation spectrum of HCF excited at 25 μ s delay after the photolysis of CHFBr₂ in the presence of 14.0 Torr argon at room temperature in the range of 19100–20680 cm⁻¹ is depicted in Figure 1. The 25 μ s delay was chosen to minimize the effects of the scattered light and allow the thermalization of the sample. The position and structure of the spectrum agrees well with the previous works^{22,25,36} and can be assigned to be the K structure of $\tilde{A}^1A''(030) \leftarrow \tilde{X}^1A'(000)$ and $\tilde{A}^1A''(020) \leftarrow \tilde{X}^1A'(000)$ transitions of the HCF transient.

The excitation dye laser, operating with Coumarin 503 at 492.70 nm (20 296.3 cm⁻¹), was used to pump the Q subband of $\tilde{A}^1A''(03^0) \leftarrow \tilde{X}^1A'(00^0)$ transition for the kinetic study. The observed time-resolved fluorescence signal of HCF(\tilde{A}^1A'') quenched by *n*-C₆H₁₄ is illustrated in Figure 2a. The nature of the exponential decays is demonstrated by the semilogarithmic plots in Figure 2b where the solid line is the result of linear least-squares fitting corresponding to more than a 100 ns delay from the maximum point to reduce the disturbance caused mainly by laser scattering light. This plot clearly shows a single

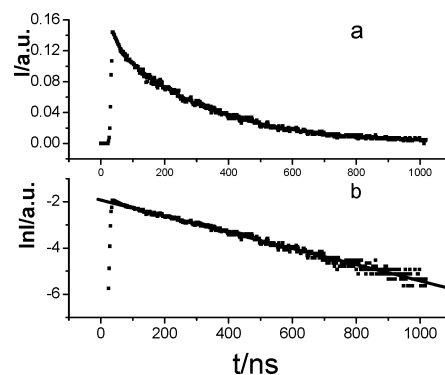


Figure 2. Typical total time-resolved fluorescence decay signal of HCF(\tilde{A}^1A'') excited at 492.70 nm quenched by C₆H₁₄ (a) and its semilogarithmic plot (b). (■) experimental data and (—) fitting result.

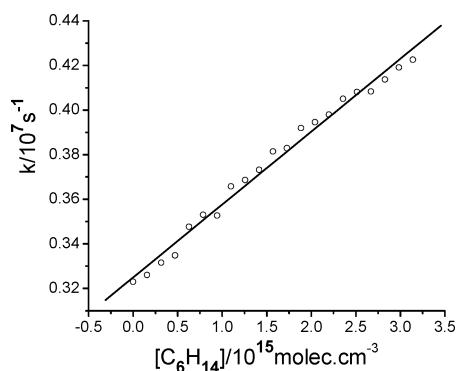


Figure 3. Plot of the pseudo-first-order rate constant k' for the quenching of HCF(\tilde{A}^1A'') as a function of the concentration of C₆H₁₄.

exponential decay phenomenon. The experimentally monitored decay curve was fitted to

$$I = I_0 \exp(-k't) \quad (1)$$

where k' is the pseudo-first-order rate coefficient. The values of k' at different partial pressures of quencher were derived from the similar plots to those illustrated in Figure 2. In the experiments, there are background gases (including argon, CHFBr₂, and some other photolysis fragments) beside the quencher. Therefore, the pseudo-first-order rate coefficient k' should be expressed as

$$k' = k_q[Q] + \sum_i k_i[M_i] + k_f \quad (2)$$

where k_q represents the quenching rate constant including the chemical reaction of HCF(\tilde{A}^1A'') with the quencher (denoted as Q) and the transition of $\tilde{A}^1A''(030)$ to other state caused by collision with Q , k_i is the collision quenching constant of HCF(\tilde{A}^1A'') by the background gases, and k_f represents the Einstein spontaneous emission coefficient of \tilde{A}^1A'' . In the present work, the background gases and total pressure were constant in all experiments, so the first-order rate coefficient is proportional to the concentration of the added quenchers. The slope coefficient is the quenching rate constant k_q and the intercept is the sum of the quenching rate constants by various background gases and Einstein spontaneous emission coefficient k_f , as shown in Figure 3.

The measured quenching rate coefficients are converted to the effective quenching cross sections σ_q by the relation

$$\sigma_q = k_q/\langle v \rangle \quad (3)$$

TABLE 1: Quenching Rate Constants k_q and Cross Sections σ_q of HCF(\tilde{A}^1A'') Radicals by Some Alkane and Alcohol Molecules Measured in This Work at 293 K

quencher	$k_q/10^{-10}\text{cm}^3\text{molec}^{-1}\text{s}^{-1}$	$\sigma_q/10^{-2}\text{nm}^2$
CH ₄	≤ 0.23	≤ 4.4
C ₂ H ₆	0.77 ± 0.12	12.4 ± 1.9
C ₃ H ₈	1.44 ± 0.16	21.6 ± 2.4
<i>n</i> -C ₄ H ₁₀	1.92 ± 0.10	27.4 ± 1.5
<i>n</i> -C ₆ H ₁₄	3.40 ± 0.27	75.1 ± 6.0
<i>n</i> -C ₅ H ₁₂	2.51 ± 0.30	35.0 ± 4.2
<i>n</i> -C ₆ H ₁₄	3.27 ± 0.17	43.5 ± 2.3
<i>n</i> -C ₇ H ₁₆	3.85 ± 0.25	51.9 ± 3.4
<i>n</i> -C ₈ H ₁₈	4.51 ± 0.19	60.1 ± 2.5
CH ₃ OH	2.91 ± 0.11	46.4 ± 1.8
C ₂ H ₅ OH	3.78 ± 0.42	56.3 ± 6.2
<i>n</i> -C ₃ H ₇ OH	4.95 ± 0.41	70.7 ± 5.9
<i>n</i> -C ₄ H ₉ OH	6.06 ± 0.40	84.3 ± 5.6

where the averaged relative kinetic velocity is

$$\langle v \rangle = (8kT/\pi\mu)^{1/2} \quad (4)$$

In the equation above, k is the Boltzmann constant, T is the absolute temperature, and μ is the reduced mass of the collision partners. A summary of the observed quenching rate coefficients and cross sections are listed in Table 1. The data in Table 1 are quoted with 2σ experimental estimates for the uncertainty.

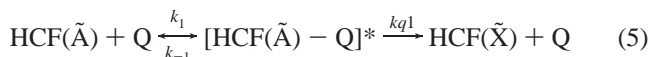
Discussion

It can be seen in Table 1 that the quenching rate constants of HCF(\tilde{A}^1A'') by alcohol and alkane molecules increase steadily with the number of C–H bond contained in these molecules, whereas the quenching of HCF(\tilde{A}^1A'') by alcohol is much more effective than that by the corresponding alkane molecules. This result is very similar to those of NCO, HCCl, and CCl₂ which have been investigated in our lab.^{55–57}

The quenching process of the excited state radical is very complicated, involving not only physical quenching but also chemical reaction. Although we could not obtain the precise mechanism just from the collision removal rate constants of HCF(\tilde{A}^1A''), we may achieve some reasonable conclusions by qualitative analysis. There have been a number of attempts to correlate the observed rate constants for collision induced electronic quenching of small molecules with the involved molecular parameters. Strong electron transfer from HCF to the quencher described by the harpooning mechanism^{58,59} cannot occur in the present case because of the large negative electron affinity of the fully saturated hydrocarbons. Selwyn and Steinfeld⁶⁰ derived a nonresonant energy transfer model which correlates the quenching cross section with reduced mass, μ , the Lennard-Jones collision radius, R , the ionization potential, IP, and polarizability α of the quenching molecule: $\sigma \propto \mu^{1/2}(\text{IP})_Q \alpha_Q R^{-3}$. With the model, Thayer and Yardley⁶¹ further induced the influence of and the permanent dipole moments. However, this model cannot account for the quenching data of our experiment according to our calculation.

The measured quenching cross sections of HCF(\tilde{A}^1A'') by alkanes and alcohols are very large and have the same magnitude as those proposed by hard sphere collision model, indicating that the long-range attractive forces between HCF(\tilde{A}^1A'') and the collision partners might have important role in the entrance channel of the quenching processes. In the collision complex model proposed in refs 62–65, the collision partners will form an excited-state complex first resulting from the long-range multipole attractive forces. During the residence time, the complex dissociates to the electronic ground-state HCF(\tilde{X}^1A')

and the quenchers through the energy transfer in different degrees of freedom form products by chemical reaction or dissociate back to the collision partners themselves. The scheme of the process can be expressed as following:



The effective attractive potential in the collision process could be expressed using the most favorable orientation method as⁶²

$$V_{\text{eff}} = \frac{Eb^2}{R^2} - \frac{C_3}{R^3} - \frac{C_4}{R^4} - \frac{C_6}{R^6} - \frac{C'_6}{R^6}$$

or using the averaged orientation method as⁶⁶

$$V_{\text{eff}} = \frac{Eb^2}{R^2} - \frac{C_6}{R^6} - \frac{C_8}{R^8} - \frac{C'_6}{R^6} - \frac{C_6}{R^6}$$

E is the initial kinetic energy at infinite separation, b is the impact parameter, and R is the distance between the centers of the masses of the quenched species and the quencher. The C_n coefficients represent the attractive terms due to multiple interactions corresponding to dipole–dipole, dipole–quadrupole, dipole–induced dipole, and dispersion forces, respectively. The expressions for these are given in refs 63 and 66. In a collision at a particular kinetic energy E , there exists an impact parameter b_0 at which the maximum of the effective potential is just equal to E , and only for $b < b_0$ the collision complex between collision partners can be formed. So the cross section for complex formation at this kinetic energy can be calculated by

$$\sigma'_{\text{eff}}(E) = \pi b_0^2(E)$$

Thus, the thermally averaged complex formation cross section at temperature T is

$$\sigma_{\text{eff}} = \frac{1}{(kT)^2} \int_0^\infty \sigma'_{\text{eff}}(E) E \exp\left(-\frac{E}{kT}\right) dE$$

The quenching cross section σ_q observed in the experiments includes the outcome (5) and (6); thus, it is equal to that of complex formation times a probability P , viz., $\sigma_q = P \sigma_{\text{eff}}$

$$\text{where } P = \frac{kq1 + kq2}{k_{-1} + kq1 + kq2} \quad (7)$$

The values for the dipole moments, μ , quadrupole moments, Q , polarizabilities, α , and ionization potentials, IP, of HCF(\tilde{A}^1A'') and collision partners required for the calculation are given in Table 2 together with the calculated cross-sections for complex formation and the probability P at 293 K. The values of the appropriate molecular parameters were taken from various literature sources (see Table 2) and those of HCF(\tilde{A}^1A'') were computed by CASSCF(8,8,nroot=2)/6-311++G** with Gaussian 98 package⁶⁷ which can give a good description of the excited-state HCF(\tilde{A}^1A'').

As is shown in Table 2, the dipole moment of alcohol molecule is usually much larger than that of the corresponding alkane, so that the long-range attractive forces between HCF(\tilde{A}^1A'') and alcohols are much stronger than those between HCF(\tilde{A}^1A'') and alkanes. According to the collision complex model, the formation cross sections of the complex of HCF(\tilde{A}^1A'') with alcohols would be much larger than those of

TABLE 2: Calculated Collision Complex Formation Cross Sections σ_{cf} of $\text{HCF}(\tilde{\text{A}}^1\text{A}'')$ with Quenchers and Parameters Used in the Calculations (α in 10^{-24} cm^3 and Q in 10^{-26} esu cm^3) at 293 K

quencher	$\mu(D)^a$	α^a	Q^b	IP ^a (eV)	σ_q (10^{-2} nm^2)	calc. σ_{cf} (10^{-2} nm^2)			
						max. ^c	P	ave. ^d	P
CH ₄	0.00	2.59	0.00	12.63	4.4	74.4	0.06	70.1	0.06
C ₂ H ₆	0.00	4.47	0.65	11.52	12.4	93.3	0.13	83.5	0.15
C ₃ H ₈	0.08	6.37	1.50	10.94	21.6	113.3	0.19	94.2	0.23
<i>n</i> -C ₄ H ₁₀	0.03	8.20	2.00	10.53	27.4	121.1	0.23	102.3	0.27
<i>n</i> -C ₅ H ₁₂	0.10	9.99	2.60	10.28	35.0	134.2	0.26	109.5	0.32
<i>n</i> -C ₆ H ₁₄	0.05	11.9	3.00	10.13	43.5	139.7	0.31	115.9	0.38
<i>n</i> -C ₇ H ₁₆	0.10	13.7	3.50	9.93	51.9	149.3	0.35	121.5	0.43
<i>n</i> -C ₈ H ₁₈	0.08 ^e	15.9 ^e	3.90 ^e	9.80 ^e	60.0	155.6	0.39	127.5	0.47
CH ₃ OH	1.70	3.29	0.50	10.84	46.4	180.4	0.26	100.4	0.46
C ₂ H ₅ OH	1.69	5.11	1.65	10.49	56.3	192.3	0.29	107.8	0.52
<i>n</i> -C ₃ H ₇ OH	1.68	6.74	2.40	10.22	70.7	200.1	0.35	113.7	0.62
<i>n</i> -C ₄ H ₉ OH	1.66	8.88	3.00	9.99	84.3	207.2	0.41	120.3	0.70
HCF($\tilde{\text{A}}$)	1.08 ^f	3.00 ^f	0.88 ^f	7.53 ^g					

^a Reference 68. ^b Reference 69. ^c Calculated using the most favorable orientation method. ^d Calculated using the averaged orientation method. ^e Estimated following refs 38 and 69 and other analogous molecule. ^f Computed with Gaussian 98 at CASSCF(8,8,root=2)/6-311++G** level. ^g Reference 70.

alkanes, Therefore, it can be seen the alcohols are much effective for the quenching of $\text{HCF}(\tilde{\text{A}}^1\text{A}'')$ than the alkanes. Table 2 also shows that the probabilities P for alcohols are generally larger than that for alkanes and they both increase steadily with increasing number of C–H bonds contained in these molecules.

For the quenching process of the electronically excited radical $\text{HCF}(\tilde{\text{A}}^1\text{A}'')$, the total available energy of the collision complex is mainly contributed by the energy of $\text{HCF}(\tilde{\text{A}}^1\text{A}'')$ because it is much greater than that of the alkane or alcohol molecule. Therefore, it can be considered that the total available energies of the complexes are similar. During the residence time of the complex, the energy will be redistributed among the various internal freedom degrees. When the complex dissociates to form physical quenching products, the electronic to vibrational energy transfer will occur between the electronic state of $\text{HCF}(\tilde{\text{A}}^1\text{A}'')$ and some certain kinds of vibrational modes of the quencher. Generally, the appropriate vibrational modes for energy transfer will grow up steadily with the increasing number of the C–H bonds contained in the analogous molecules. For a given total energy, it can be expected that the rate constant $kq1$ will be bigger for a larger molecule than that for an analogous smaller one.

As has been mentioned above, many studies have shown the singlet excited-state carbenes undergo bond insertion or addition reaction in the quenching processes.^{2,5,9–21} If this is the case, then it does not exhibit marked variations with the type of bond or substitute groups involved. Our results establish that substitute groups and steric factors do not affect removal rate constants of $\text{HCF}(\tilde{\text{A}}^1\text{A}'')$ in the presence of alkanes and alcohols, which is consistent with the addition or insertion mechanism. As is plotted in Figure 5, the quenching rate constants of $\text{HCF}(\tilde{\text{A}}^1\text{A}'')$ by alkanes and alcohols increase almost linearly with the number of C–H bonds contained in the analogous molecules, and there are no remarkable variations with the type of C–H bonds. In present work, the quenchers are all fully saturated hydrocarbons; therefore, only bond insertion reaction can possibly occur.

If the reactive species is known to react with a series of organic compounds via similar mechanistic pathway, it may be expected that there will exist relationships between the structural and physical properties of the molecule and its reactivity. Many experimental studies indicate a general trend in the reactivity of radical molecule. For H-abstraction reactions, the rate constants mainly correlate with bond dissociation energy, and for addition and insertion reactions, the rate constants correlate with the ionization potential of these compounds.^{71–76} The

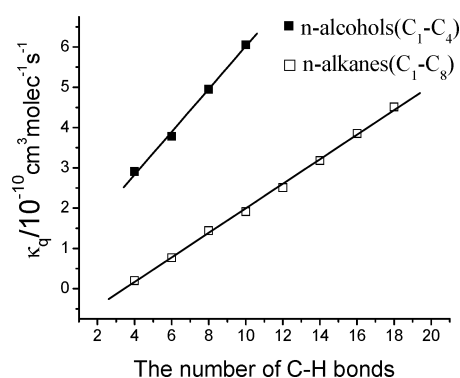


Figure 4. Dependence of the experimental rate constants σ_q for quenching of $\text{HCF}(\tilde{\text{A}}^1\text{A}'')$ by alkane and alcohol molecules on the number of C–H bonds contained in the quenchers.

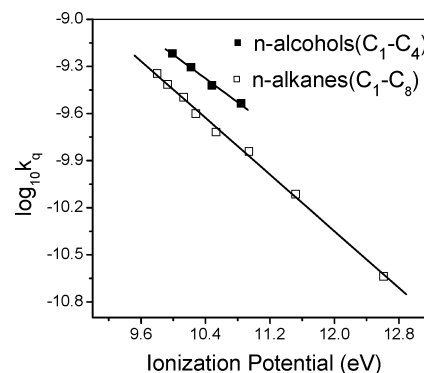


Figure 5. Dependence of the experimental quenching rate constants of $\text{HCF}(\tilde{\text{A}}^1\text{A}'')$ by alkanes and alcohols on the ionization potential of these molecules.

semilogarithmic plots of quenching rate constants of $\text{HCF}(\tilde{\text{A}}^1\text{A}'')$ to the ionization potentials of the quenchers are shown in Figure 4. The ionization potentials of the analogy molecules decrease with the increasing number of C atom contained in these molecules, whereas the reaction rate constants increase with the decrease of the ionization potential. These data have good linearity for analogous molecules and strongly support the insertion mechanism for these processes.

Since the total available energy of the complexes are similar, it can be expected that the rate constant k_{-1} will decrease with the increasing attractive forces between the collision partners in the complexes. The attractive forces between alkanes and $\text{HCF}(\tilde{\text{A}}^1\text{A}'')$ increase with the increasing number of C atoms.

Also, there is the same trend for the alcohols, although they are larger than those for alkanes. So k_{-1} should decrease with the increasing number of C atoms contained in the alkane and alcohol molecules.

According to eq 7, the rate constants and the possibilities P would exhibit the behavior as shown in Tables 1 and 2, respectively. Based on all above analysis, we consider that the quenching of HCF(\tilde{A}^1A'') by alkanes and alcohols are likely to form collision complexes due to the long-range attractive forces between the collision partners, and then it dissociates to quenching products via E–V energy transfer and insertion chemical reaction.

Conclusion

In this work, the quenching rate constants of HCF(\tilde{A}^1A'') by alkane and alcohol molecules were measured by using the LP-LIF experiments. These rate constants increase almost linearly with the increase of the number of C–H bonds contained in the analogous molecules. By analyzing the experimental results with the collision complex model, the attractive forces between the collision partners were demonstrated to play an important role in the formation of complexes between HCF(\tilde{A}^1A'') and the quenchers and the quenching process may include E–V energy transfer in the collision complex and chemical reaction via insertion mechanism.

Acknowledgment. This work was financially supported by the China National Key Basic Research Special Foundation (G1999075304), the National Natural Science Foundation of China (10032050, 20373065, 20328305), and Chinese Academy of Science (KJXC2-SW-H08).

References and Notes

- Jones, M.; Moss, R. A. *Carbenes*; Wiley: New York, 1975.
- Cheng, Y.; Meth-Cohn, O. *Chem. Rev.* **2004**, *104*, 2507–2530.
- Bertrand, G. *Carbene Chemistry: From Fleeting Intermediates to Powerful Reagents*; Fontis Media and Marcel Dekker: New York, 2002.
- Wentrup, C. *Reactive Molecules*; Wiley-Interscience: New York, 1984.
- Skell, P. S.; Garner, A. Y. *J. Am. Chem. Soc.* **1956**, *78*, 5430–5433.
- Doering, W. Y. E.; Henderson, W. A., Jr. *J. Am. Chem. Soc.* **1958**, *80*, 5274–5277.
- Wagener, R.; Wagner, H. Gg. *Ber. Bunsen-Ges. Phys. Chem.* **1990**, *94*, 1096–1100.
- Ashfold, M. N. R.; Fullstone, M. A.; Hancock, G.; Ketley, G. W. *Chem. Phys.* **1981**, *55*, 245–257.
- Langford, A. O.; Petek, H.; Moore, C. B. *J. Chem. Phys.* **1983**, *78*, 6650–6659.
- Tang, Y. N.; Rowland, F. S. *J. Am. Chem. Soc.* **1967**, *89*, 6420–6427.
- Dornhöfer, G.; Hack, W. *J. Chem. Soc., Faraday Trans. 2* **1988**, *84*, 441–450.
- Dornhöfer, G.; Hack, W. *Ber. Bunsen-Ges. Phys. Chem.* **1988**, *92*, 485–490.
- Cain, S. R.; Hoffman, R.; Grant, E. R. *J. Phys. Chem.* **1981**, *85*, 4046–4051.
- Harding, L. B.; Schlegel, H. B.; Krishnan, R.; Pople, J. A. *J. Phys. Chem.* **1980**, *84*, 3394–3401.
- Sosa, C.; Schlegel, H. B. *J. Am. Chem. Soc.* **1984**, *106*, 5847–5852.
- Moreno, M.; Lluch, J. M.; Oliva, A.; Bertran, J. *J. Phys. Chem.* **1988**, *92*, 4180–4184.
- Houk, K. N.; Rondan, N. G.; Mareda, J. *J. Am. Chem. Soc.* **1984**, *106*, 4291–4293.
- Houk, K. N.; Rondan, N. G. *J. Am. Chem. Soc.* **1984**, *106*, 4293–4294.
- Rondan, N. G.; Houk, K. N.; Moss, R. A. *J. Am. Chem. Soc.* **1980**, *102*, 1770–1776.
- Moss, R. A. *Acc. Chem. Res.* **1989**, *22*, 15–21.
- Moss, R. A. *Acc. Chem. Res.* **1980**, *13*, 58–64.
- Merer, A. J.; Travis, D. N. *Can. J. Phys.* **1966**, *44*, 1541–1550.
- Jacox, M.; Milligan, D. *J. Chem. Phys.* **1969**, *50*, 3252–3262.
- Patel, R. I.; Stewart, G. W.; Casleton, K.; Gole, J. G.; Lombardi, J. R. *Chem. Phys.* **1980**, *52*, 461–468.
- Ashfold, M. N. R.; Castano, F.; Hancock, G.; Ketley, G. W. *Chem. Phys. Lett.* **1980**, *73*, 421–424.
- Kakimoto, M.; Saito, S.; Hirota, E. *J. Mol. Spectrosc.* **1981**, *88*, 300–310.
- Butcher, R. J.; Saito, S.; Hirota, E. *J. Chem. Phys.* **1984**, *80*, 4000–4002.
- Suzuki, T.; Saito, S.; Hirota, E. *Can. J. Phys.* **1984**, *62*, 1328.
- Suzuki, T.; Hirota, E. *J. Chem. Phys.* **1986**, *85*, 5541–5546.
- Suzuki, T.; Hirota, E. *J. Chem. Phys.* **1988**, *88*, 6778–6784.
- Murray, K.; Leopold, D.; Miller, T.; Lineberger, W. *J. Chem. Phys.* **1988**, *89*, 5442–5453.
- Qui, Y.; Zhou, S.; Shi, J. *Chem. Phys. Lett.* **1987**, *136*, 93–96.
- Ibuki, T.; Hiraya, A.; Shobatake, K.; Matsumi, Y.; Kawasaki, M. *J. Chem. Phys.* **1990**, *92*, 4277–4282.
- Irikura, K.; Hudgens, J.; Johnson, R., III. *J. Chem. Phys.* **1995**, *103*, 1303–1308.
- Schmidt, T. W.; Bacskey, G. B.; Kable, S. H. *Chem. Phys. Lett.* **1998**, *292*, 80–86.
- Schmidt, T. W.; Bacskey, G. B.; Kable, S. H. *J. Chem. Phys.* **1999**, *110*, 11277–11285.
- Fan, H. Y.; Ionescu, I.; Annesley, C.; Reid, S. A. *Chem. Phys. Lett.* **2003**, *378*, 548–552.
- Fan, H. Y.; Ionescu, I.; Annesley, C.; Cummins, J.; Bowers, M. Xin, J.; Reid, S. A. *J. Phys. Chem. A* **2004**, *108*, 3732–3738.
- Fan, H. Y.; Ionescu, I.; Xin, J.; Reid, S. A. *J. Chem. Phys.* **2004**, *121*, 8869–8874.
- Ionescu, I.; Fan, H. Y.; Ionescu, E.; Reid, S. A. *J. Chem. Phys.* **2004**, *121*, 8874–8879.
- Cookson, J. L.; Hancock, G.; McKendrick, K. G. *Ber. Bunsen-Ges. Phys. Chem.* **1985**, *89*, 335–340.
- Hancock, G.; Ketley, G. W.; MacRobert, A. J. *J. Phys. Chem.* **1984**, *88*, 2104–2109.
- Tsai, C.; McFadden, D. L. *J. Phys. Chem.* **1990**, *94*, 3298–3300.
- Brownsword, R. A.; Hancock, G.; Heard, D. E. *J. Chem. Soc., Faraday Trans.* **1991**, *87*, 2283–2289.
- Hancock, G.; Ketley, G. W. *J. Chem. Soc., Faraday Trans. 2* **1982**, *88*, 1283–1291.
- Castano, F.; Ortiz de Zarate, A. *An. Quim.* **1991**, *87*, 167–173.
- Ortiz de Zarate, A.; Martinex, R.; Sanchez Rayo, M. N.; Castano, F. *An. Quim.* **1997**, *93*, 22–27.
- Hack, W.; Wagner, Hoyer, K. *Z. Phys. Chem.* **2000**, *214*, 741–752.
- Ortiz de Zarate, A.; Martinex, R.; Sanchez Rayo, M. N.; Castano, F.; Hancock, G. *J. Chem. Soc., Faraday Trans.* **1992**, *88*, 535–541.
- Brownsword, R. A.; Hancock, G.; Oum, K. W. *J. Phys. Chem.* **1996**, *100*, 4840–4847.
- Hu, C. J.; Zhu, Z. Q.; Pei, L. S.; Ran, Q.; Chen, Y.; Chen, C. X.; Ma, X. X. *J. Chem. Phys.* **2003**, *118*, 5408–5412.
- Hu, C. J.; Liu, Y. Z.; Pei, L. S.; Dai, J. H.; Chen, Y.; Chen, C. X.; Ma, X. X. *Chem. Phys.* **2003**, *289*, 389–396.
- Liu, Y. Z.; Zhang, Z. Q.; Pei, L. S.; Ran, Q.; Chen, Y.; Chen, C. X. *Chem. Phys.* **2004**, *303*, 255–263.
- Huang, C. S.; Zhu, Z. Q.; Xin, Y.; Chen, C. X.; Chen, Y. *J. Chem. Phys.* **2004**, *120*, 2225–2229.
- Gao, Y. D. Ph.D. Thesis. University of Science and Technology of China, 2001.
- Pei, L. S.; Hu, C. J.; Liu, Y. Z.; Zhu, Z. Q.; Chen, Y.; Chen, C. X. *Chem. Phys. Lett.* **2003**, *381*, 199–204.
- Liu, Y. Z. Ph.D. Thesis. University of Science and Technology of China, 2004.
- Asscher, M.; Haas, Y. *J. Chem. Phys.* **1982**, *76*, 2115–2126.
- Paul, H.; Gray, J. A.; Durant, J. L., Jr.; Thoman, J. W., Jr. *App. Phys. B* **1993**, *57*, 249.
- Selwyn, J. E.; Steinfeld, J. I. *Chem. Phys. Lett.* **1969**, *4*, 217–220.
- Thayer, C. A.; Yardley, Y. T. *J. Chem. Phys.* **1972**, *57*, 3992–4001.
- Fairchild, P. W.; Smith, G. P.; Closley, D. R. *J. Chem. Phys.* **1983**, *79*, 1795–1807.
- Trully, J. C. *J. Chem. Phys.* **1974**, *61*, 61–68.
- Zahr, G. E.; Preston, R. K.; Miller, W. H. *J. Chem. Phys.* **1975**, *62*, 1127–1135.
- Holtermann, D. L.; Lee, E. K. C.; Nanes, R. *J. Chem. Phys.* **1982**, *77*, 5327–5339.
- Hirschfelder, J. O.; Curtis, C. F.; Bird, R. B. *Molecular Theory of Gases and Liquids*; Wiley: New York, 1954.
- Frisch, M. J.; Trucks, G. W.; Schlegel, H. B.; Scuseria, G. E.; Robb, M. A.; Cheeseman, J. R.; Zakrzewski, V. G.; Montgomery, J. A., Jr.; Stratmann, R. E.; Burant, J. C.; Dapprich, S.; Millam, J. M.; Daniels, A. D.; Kudin, K. N.; Strain, M. C.; Farkas, O.; Tomasi, J.; Barone, V.; Cossi, M.; Cammi, R.; Mennucci, B.; Pomelli, C.; Adamo, C.; Clifford, S.; Ochterski, J.; Petersson, G. A.; Ayala, P. Y.; Cui, Q.; Morokuma, K.; Malick,

D. K.; Rabuck, A. D.; Raghavachari, K.; Foresman, J. B.; Cioslowski, J.; Ortiz, J. V.; Stefanov, B. B.; Liu, G.; Liashenko, A.; Piskorz, P.; Komaromi, I.; Gomperts, R.; Martin, R. L.; Fox, D. J.; Keith, T.; Al-Laham, M. A.; Peng, C. Y.; Nanayakkara, A.; Gonzalez, C.; Challacombe, M.; Gill, P. M. W.; Johnson, B. G.; Chen, W.; Wong, M. W.; Andres, J. L.; Head-Gordon, M.; Replogle, E. S.; Pople, J. A. *Gaussian 98*, revision A.7; Gaussian, Inc.: Pittsburgh, PA, 1998.

(68) Weast, R. C. *CRC Handbook of Chemistry and Physics*, 80th ed.; CRC Press: Boca Raton, FL, 2000; Chapter 9.

(69) Stogryn, D. D.; Stogryn, A. P. *Mol. Phys.* **1966**, *11*, 371–393.

(70) Copeland, R. A.; Dyer, M. J.; Closley, D. R. *J. Chem. Phys.* **1985**, *82*, 4022–4032.

(71) Huie E.; Herron, J. T. *Prog. React. Kinet.* **1975**, *8*.

(72) Cvetanovic, R. J. *Advances in Photochemistry*; John Wiley & Sons: New York, 1963.

(73) Cvetanovic, R. J. *J. Chem. Phys.* **1959**, *30*, 19–26.

(74) Atkinson, R.; Pitts, J. N., Jr. *J. Chem. Phys.* **1977**, *67*, 2492–2495.

(75) Gaffney, J. S.; Levine, S. Z. *Int. J. Chem. Kinet.* **1979**, *11*, 1197–1209.

(76) Atkinson, R. *Chem. Rev.* **1986**, *86*, 69–201.